PERGAMON

Chemical Engineering Science 58 (2003) 979–985

Chemical Engineering Science

www.elsevier.com/locate/ces

Absolute quantum yields in photocatalytic slurry reactors

Rodolfo J. Brandi, Miguel A. Citroni, Orlando M. Alfano, Alberto E. Cassano*

INTEC (Universidad Nacional del Litoral-CONICET), Güemes 3450, (3000) Santa Fe, Argentina

Abstract

Photocatalysis in slurry reactors have the particular characteristic that the reacting medium not only absorbs but also scatters photons and both phenomena occurs simultaneously. When this is the case, typical methods used in classical photochemistry such as homogeneous actinometry are useless because they cannot take into account radiation scattering. Consequently present methods in use always underestimate quantum yields calculations. A method has been developed to produce absolute values of photocatalytic quantum yields in slurry reacting systems employing titanium dioxide and near UV radiation. The new procedure resorts to the rigorous solution of the radiative transfer equation inside the reaction space in order to obtain the *true* value of the photonic absorption rate. Employing monochromatic light, values for the photocatalytic decomposition of phenol and 1,4-dioxane are reported under precisely defined conditions. The method can be used to compare reactivities of different catalysts or, for a given catalyst, reactivities with different compounds regardless the reactor shape, size or configuration.
© 2003 Elsevier Science Ltd. All rights reserved.

Keywords: Photocatalysis; Absolute quantum yield; Radiation; Reaction engineering; Modeling; Remediation

1. Introduction

Photocatalytic reactions are the result of a light activated process by which an appropriate semiconductor upon irradiation with the required energy can generate electrons and holes that, afterwards, can participate in oxidation–reduction reactions. One of the most important applications of these processes consists in the use of these catalytic systems for treating polluted water and air environments. In these photocatalytic reactions, in the absence of mass transfer limitations, the initiation step is at all times a function of the local volumetric rate of photon absorption (LVRPA) that must be always known to formulate the rate. Many of these reactions are operated in fluid systems where the catalyst is a suspension of small size, solid particles; then, the system is heterogeneous and evaluation of the light distribution becomes difficult due to the concomitant presence of radiation absorption and scattering.

Homogeneous photochemistry uses actinometry to supply, at least partially, this information. This is a very crude approximation even in homogeneous systems because it only measures the amount of photons arriving at the reactor window for radiation entrance and does not provide the exact amount of photons that are absorbed in the actual reacting system—that is different from the actinometer solution. Nor does actinometry provide information about the spatial distribution of the absorbed energy, an important fact because reaction rates non-uniformities are intrinsic of photochemical systems. Thus, usually, averaged photon absorption rates are used for calculating spatially distributed reaction rates, a procedure that cannot render precise kinetic information. In heterogeneous systems the situation is nothing but worst because the homogeneous actinometer cannot account for photon scattering and consequently the chemical measurements provide, at the best, some sort of global, upper limit for the photon absorption rate.

A very typical property of photochemical systems is the quantum yield. Employing monochromatic radiation, the quantum yield is defined as (Calvert & Pitts, 1966)

$$\Phi_\lambda = \frac{[\text{Volumetric reaction rate of species (event) } i]}{[\text{Volumetric rate of } \lambda - \text{photons absorption by the involved reactant}]} = \frac{\langle R_\lambda \rangle_{V_R}}{\langle e^a_\lambda \rangle_{V_R}}. \quad (1)$$

Note that both the numerator and the denominator indicate volume-averaged rates.

* Corresponding author. Fax: +54-342-4559185.
E-mail address: acassano@ceride.gov.ar (A. E. Cassano).

0009-2509/03/$ - see front matter © 2003 Elsevier Science Ltd. All rights reserved.
doi:10.1016/S0009-2509(02)00638-3

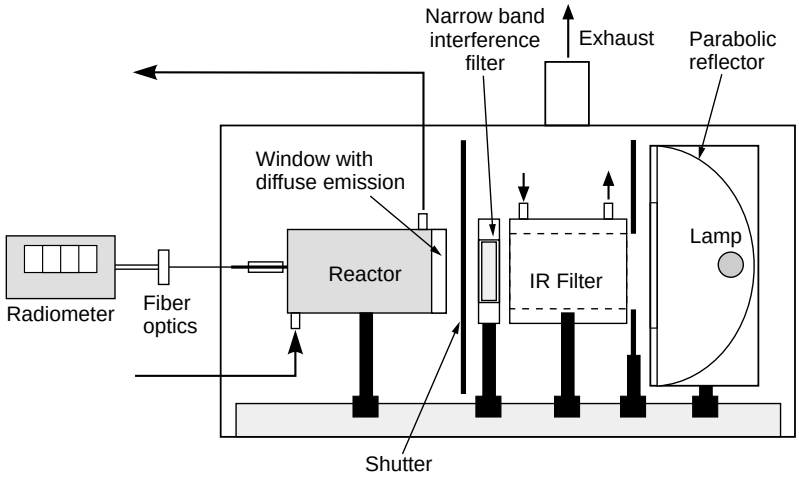

Fig. 1. Schematic representation of the UV detector, photoreactor, and emitting system.

The same definition has been applied to heterogeneous systems. In these cases it is more evident that the resulting "absorbed photons" provided by actinometry to the denominator of Eq. (1) is only an upper limit and, consequently the figure gives an approximate lower limit for the quantum yield. Recognizing this limitation it is often said that employing homogeneous actinometry results are just *apparent* quantum yields. However, since actinometry actually gives a precise value of the photons impinging the window of radiation entrance, circumventing the problem, the definition is sometimes changed to use the radiation flux arriving at such a surface. Then

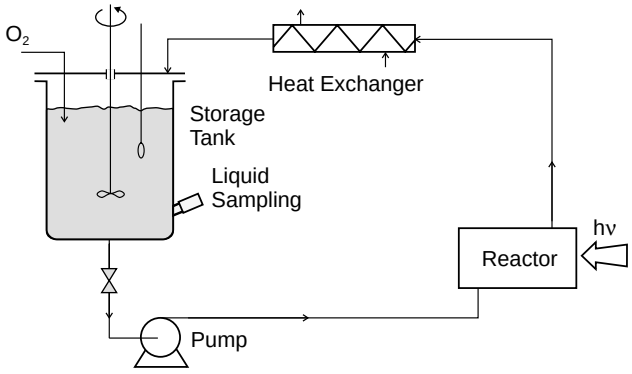

Fig. 2. Flow sheet of the experimental device. (Adapted from Cabrera, Negro, Alfano, & Cassano, 1997.)

$$\Phi_{\lambda}^{\mathrm{App}} = \frac{[\text{Reaction rate of species (event) } i]}{[\text{Rate of } \lambda - \text{photons arriving at the reactor surface}]} = \frac{\langle R_{\lambda}\rangle_{V_R} V_R}{\langle q_{\lambda}\rangle_{A_{\mathrm{inc}}} A_{\mathrm{inc}}}. \quad (2)$$

In our opinion, one must recognize that the volumetric rate of photon absorption in a heterogeneous system is rather difficult to measure with conventional kinetic experiments. One need to use an experimental device that permits the exact measurement of the arriving photons and, at the same time, an account for all those photons that are escaping from the reactor boundaries, including back scattering at the window of radiation entrance. This is not impossible but achievable with accuracy only in very special cases. On the other hand it is normally possible to build a simple reactor that is amenable of precise mathematical modeling and, applying good chemical and radiation engineering principles, solve the radiative transfer equation (RTE) for such a reactor and calculate the denominator of Eq. (1). This paper shows the method and indicates the additional independent measurements that are needed to apply the RTE to the particular experimental setup.

2. Experimental reactor (Figs. 1 and 2)

The proposed reactor for these experiments is a cylindrical tube made of Pyrex glass that has two flat windows, one of which must be made of good quality quartz. The cylinder has two ports for the reacting solution entrance and exit. The external side of the quartz window, upon abrasion with HF, has the texture of ground glass. This is one important feature: with this very modest modification it is possible to get *diffuse* irradiation inside the reactor with very significant consequences in the mathematical modeling. The change in the surface must be made on the outside to avoid an enhancement of the typical fouling properties of titanium dioxide suspensions. The reactor length is 10 cm. A rather long reactor will ensure that absorption and scattering along the characteristic radiation path length will preclude the arrival of photons at the second window. In this way we can have a *non-reflecting* boundary condition at the plate

opposite to the one for radiation entrance. The reactor volume is 210 cm^3. A shutter, placed in front of the reactor window permitted to decide on the exact starting time of the reaction once steady state operating conditions has been reached.

The photoreactor is part of a recycling system that has a storage tank made of glass. The liquid flow in the closed circuit is provided by a high flow rate recirculating pump also made of glass and Teflon. Connecting lines are made of glass. The tank with a volume slightly larger than 2000 cm^3 permits the following operations: (1) temperature measurements, (2) sampling of the liquid and the gas phase, and (3) continuous feeding of oxygen at constant pressure.

The reactor window is irradiated by means of a tubular lamp (Medium pressure, Mercury arc, G. E. 360 UA-3) having a nominal power consumption of 360 W. This lamp has a total emission of 61.4 W and significant peaks at 313 and 365 nm. It was placed at the focal axis of a parabolic reflector made of mirror polished aluminum with Alzak treatment. Monochromatic light was obtained by interposing between the illuminating system and the reactor window, narrow band interference filters (CVI: F10-313.0-3-2.00, peak at 313 nm and F10-365.0-4-2.00, peak at 365 nm). To protect the filters from emission at longer wavelengths, an infrared absorbing filter was placed between the lamp and the filter holder.

A calibrated photodiode detector (GaAsP type, SED005 from International Light) with a band pass filter connected with a quartz optical fiber to a UV radiometer (IL1745 UV Curing Radiometer from International Light), was placed by the reactor window opposite to the one of radiation entrance. It permitted monitoring of: (1) the lamp emission and (2) the light transmission conditions of both reactor windows as a consequence of the unavoidable fouling produced by the catalyst.

The following operating conditions were ensured: (1) very good mixing in the reactor in order to simplify the mass balance, facilitate uniform distribution of the catalyst throughout and avoid the existence of mass transfer limitations, (2) very good reproducibility in the radiation flux arriving at the reactor window, (3) very high recirculating flow rate to improve mixing and produce differential conversion per pass in the reactor (again to simplify the mass balance), (4) well mixing conditions in the tank, (5) excess oxygen demand always present in the reactor, and (6) absence of gas leaks everywhere.

3. Theoretical background for the analysis of results

The proposed method is based on the following procedures: (i) measure the reaction rate in the numerator of Eq. (1) with experiments. In order to minimize the effect of adsorption on the catalyst by reaction intermediates or products, initial reaction rates have been measured, and (ii) calculate the denominator of Eq. (1) by solving the radiative transfer equation inside the reactor.

3.1. The reaction rate

Cabrera, Negro, Alfano, & Cassano (1997) have shown that when the following conditions are fulfilled: (1) the reactor is well mixed, (2) the tank is well mixed, (3) the system is isothermal, and (4) the reactor has differential operation, the following equation represents the mass balance for the batch recycling system:

$$\langle R_\lambda(\underline{x},t)\rangle_{V_R} = \varepsilon_L \frac{V_T}{V_R}\left[\left.\frac{\mathrm{d}C(t)}{\mathrm{d}t}\right|_{\mathrm{Tk}}\right]. \tag{3}$$

Using experimental information, initial rates are calculated according to

$$\langle R_\lambda(\underline{x},t)\rangle_{V_R}^{t\to 0} = \varepsilon_L \frac{V_T}{V_R}\lim_{t\to 0}\left[\left.\frac{\Delta C(t)}{\Delta t}\right|_{\mathrm{Tk}}\right]. \tag{4}$$

3.2. The local volumetric rate of photon absorption

In radiation field and photoreaction engineering theory (Özisik, 1973; Cassano, Martín, Brandi, & Alfano, 1995) it was shown that the rate of λ-photon transport with direction $\underline{\Omega}$ along a distance s is given by

$$\frac{\mathrm{d}I_{\lambda,\underline{\Omega}(\theta,\phi)}(\underline{x},t)}{\mathrm{d}s} = -\underbrace{\kappa_\lambda(\underline{x},t)I_{\lambda,\underline{\Omega}(\theta,\phi)}(\underline{x},t)}_{\text{ABSORPTION}} - \underbrace{\sigma_\lambda(\underline{x},t)I_{\lambda,\underline{\Omega}(\theta,\phi)}(\underline{x},t)}_{\text{OUT-SCATTERING}} + \underbrace{j^e_\lambda(\underline{x},t)}_{\text{EMISSION}} + \underbrace{\frac{\sigma_\lambda(\underline{x},t)}{4\pi}\int_{\Omega'=4\pi} p[\underline{\Omega}'(\theta',\phi')\to\underline{\Omega}(\theta,\phi)]I_{\lambda,\underline{\Omega}(\theta,\phi)}(\underline{x},t)\,\mathrm{d}\Omega'(\theta',\phi')}_{\text{IN-SCATTERING}}. \tag{5}$$

This equation is valid for elastic and multiple scattering. When the scattering coefficient (σ_λ) bears a linear dependence with the solid concentration it is said that scattering is independent. In photocatalysis we normally have elastic, multiple and independent scattering. Moreover, since the reaction is carried out at ambient temperature, emission is safely neglected. If we can get values of the monochromatic specific intensities as a function of position and direction, the following operations are possible:

$$G_\lambda(\underline{x},t) = \int_\Omega I_{\lambda,\underline{\Omega}(\theta,\phi)}(\underline{x},t)\sin\theta\,\mathrm{d}\theta\,\mathrm{d}\phi \tag{6}$$

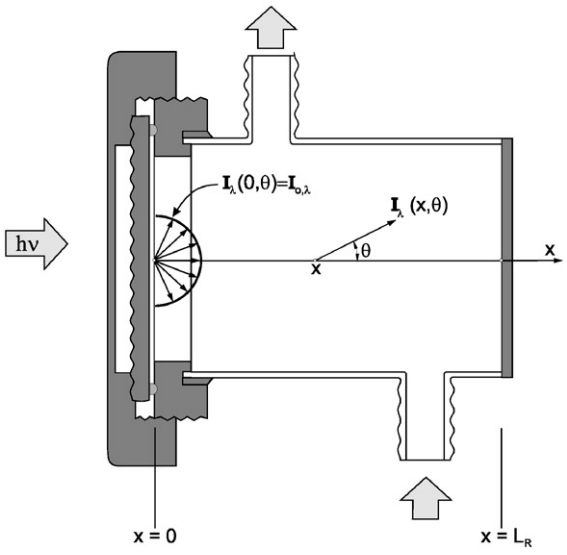

Fig. 3. Geometry of the photocatalytic reactor. (Adapted from Cassano et al., 1995.)

The incident radiation,

$$e^a_\lambda(\underline{x},t)=\kappa_\lambda(\underline{x},t)G(\underline{x},t) \quad \text{The LVRPA,} \tag{7}$$

$$\langle e^a_\lambda(\underline{x},t)\rangle_{V_R}=\frac{1}{V_R}\int_{V_R}\kappa_\lambda(\underline{x},t)G(\underline{x},t)\,\mathrm{d}V \quad \text{The VRPA.} \tag{8}$$

Eq. (8) is needed for the denominator of Eq. (1). To solve this equation for a particular control volume we need some information as follows: (i) the boundary condition on each limiting surface of the control volume (V_R), (ii) the value of p (the phase function for scattering distribution), and (iii) the absorption and scattering coefficients (κ_λ and σ_λ).

3.3. The one-dimensional model

Because of the existing ground glass at the window of photon entrance the incoming radiation is diffuse; then, there exists azimuthal symmetry. With this symmetry the radiation can be modeled with one spatial coordinate (x) and just one angular coordinate (θ) for the directional characterization of the propagation rays (Fig. 3). This fact and the adopted reactor length permit to write the RTE and the boundary conditions as follows:

$$\cos\theta\frac{\partial I_\lambda(x,\theta)}{\partial x}+(\kappa_\lambda+\sigma_\lambda)I_\lambda(x,\theta)$$

$$=\frac{\sigma_\lambda}{2}\int_{\theta'=0}^{\theta'=\pi}I_\lambda(x,\theta')p(\theta,\theta')\sin\theta'\,\mathrm{d}\theta', \tag{9}$$

$$I_\lambda(0,\theta)=I^0_\lambda,\quad 0\leqslant\theta<\pi/2$$

(Photons moving forward), (10)

$$I_\lambda(L_R,\theta)=0,\quad \pi/2<\theta\leqslant\pi$$

(Photons moving backwards). (11)

Diffuse radiation permits to consider incoming intensities at $x=0$ independent of direction [Eq. (10)]. Thus, I^0_λ is a single value that can be easily calculated if the radiation fluxes at the wall of radiation entrance are calculated or measured. Eq. (11) profits from the fact that for the used catalyst concentration and reactor length, no radiation is arriving at $x=L_R$ (hence, the non-reflecting boundary condition).

Eq. (9) with B.C. (10) and (11) can have a numerically accurate solution with the discrete ordinate method (Duderstadt & Martin, 1979). But before that, we need values for κ_λ, σ_λ, p and I^0_λ. Values for κ_λ and σ_λ were obtained by Cabrera, Alfano, and Cassano (1996). These values were corrected in 1998 by the same group of authors to include more reliable values obtained with better information concerning the phase function. Unpublished values for Degussa P 25 are

$$313\text{ nm},\quad \kappa_\lambda=18722\text{ cm}^2\text{ g}^{-1},\quad \sigma_\lambda=50418\text{ cm}^2\text{ g}^{-1},$$

$$365\text{ nm},\quad \kappa_\lambda=2548\text{ cm}^2\text{ g}^{-1},\quad \sigma_\lambda=52547\text{ cm}^2\text{ g}^{-1}.$$

It can be seen that the scattering coefficient is much larger than the absorption one, meaning that any form of analysis that does not take into account scattering will be usually in a rather serious error. Working with a special type of flat plate reactor and precise radiometer measurements, Brandi, Alfano, and Cassano (1999) have shown that isotropic scattering is the phase function that better represents scattering by titanium dioxide, particularly when the Degussa P 25 variety is employed. Consequently, it is safe to adopt that $p=1$.

3.4. The radiation boundary condition

The arriving radiation at the wall of radiation entrance was measured with homogeneous actinometry employing potassium ferrioxalate and using standard procedures (Murov, Carmichael, & Hug, 1993).

For the homogeneous reaction and the one-dimensional model, the RTE is

$$\mu\frac{\mathrm{d}I_{\lambda,\underline{\Omega}}(x,t)}{\mathrm{d}x}+\kappa_\lambda(x,t)I_{\lambda,\underline{\Omega}}(x,t)=0. \tag{12}$$

This equation corresponds to a model having azimuthal symmetry due to the existence of the ground glass modification in the plate of radiation entrance (that produces diffuse radiation). Integrating Eq. (12):

$$I_{\lambda,\underline{\Omega}}(x,\mu,t)=I^0_\lambda\exp\left[-\frac{\kappa_\lambda(t)}{\mu}x\right]. \tag{13}$$

Then, the LVRPA becomes

$$e^a_\lambda(x,t)|_{\mathrm{Act}}=2\pi\kappa^{\mathrm{Fe}^{3+}}_\lambda(t)\int_{-1}^{1}I_{\lambda,\underline{\Omega}}(x,\mu',t)\,\mathrm{d}\mu'$$

$$=2\pi\kappa^{\mathrm{Fe}^{3+}}_\lambda(t)I^0_\lambda E_2[\kappa^{\mathrm{tot}}_\lambda(t)x], \tag{14}$$

Table 1
Boundary conditions

Boundary conditions	
I_λ^0 at 313 nm	2.187×10^{-10} einstein cm^{-2} s^{-1} sr^{-1}
I_λ^0 at 365 nm	4.997×10^{-10} einstein cm^{-2} s^{-1} sr^{-1}

where the nth exponential integral has been defined as follows (Siegel & Howell, 1992):

$$E_n(z) = \int_0^1 \mu^{n-2} \exp\left[-\frac{z}{\mu}\right] \mathrm{d}\mu. \tag{15}$$

The mass balance for the actinometer reaction is

$$\langle R_\lambda^{\mathrm{Act}}(x,t)\rangle_{L_R} = \frac{V_T}{V_R}\left[\left.\frac{\mathrm{d}C^{\mathrm{Fe}^{2+}}(t)}{\mathrm{d}t}\right|_{\mathrm{Tk}}\right] = \Phi_\lambda^{\mathrm{Act}}\langle e_\lambda^a|_{\mathrm{Act}}\rangle_{L_R}. \tag{16}$$

In Eq. (16) the reaction rate is expressed as a first-order process with respect to the LVRPA and $\Phi_\lambda^{\mathrm{Act}}$ is the monochromatic, overall quantum yield for the actinometer reaction. At low reactant conversions this reaction may be assumed independent of the ferric and ferrous salts concentrations that, as indicated by Eq. (14) participate in the value of e_λ^a. For the one-dimensional model, in a well-mixed reactor and for a reactor of constant cross-sectional area, the volume-average required by Eq. (16) is taken over the reactor length. Calculating the reactor length-average of Eq. (14):

$$\begin{aligned}\langle e_\lambda^a|_{\mathrm{Act}}\rangle_{L_R} &= \frac{1}{L_R}\int_0^{L_R} \left.e_\lambda^a\right|_{\mathrm{Act}} \mathrm{d}x \\ &= \frac{1}{L_R} 2\pi\kappa_\lambda^{\mathrm{Fe}^{3+}}(t) I_\lambda^0 \int_0^{L_R} E_2[\kappa_\lambda^{\mathrm{tot}}(t)x]\,\mathrm{d}x \\ &= \frac{\pi I_\lambda^0}{L_R}\frac{\kappa_\lambda^{\mathrm{Fe}^{3+}}(t)}{\kappa_\lambda^{\mathrm{tot}}(t)}.\end{aligned} \tag{17}$$

The last result follows because: $\int E_n(z)\,\mathrm{d}z = -E_{n+1}$, $E_3(0) = \frac{1}{2}$, and $\lim_{z\to\infty} E_3(z) \to 0$. The last equation can be applied because the product $\kappa_\lambda^{\mathrm{tot}} L_R$, at 313 and 365 nm, is large.

When $t \to 0$, radiation absorption by the Fe^{2+} salt is negligible and radiation absorption by the Fe^{3+} is very well defined and equal to the total absorption coefficient. Working with initial rates, from Eqs. (16) and (17), the following very simple result is obtained:

$$I_\lambda^0 = \frac{V_T}{\pi A_R \Phi_\lambda^{\mathrm{Act}}} \lim_{t\to t_0}\left(\frac{C^{\mathrm{Fe}^{2+}}}{t - t_0}\right). \tag{18}$$

For low reactant (Fe^{3+}) conversion a plot of the concentration of Fe^{2+} vs. time gives a straight line. For the one-dimensional model Eq. (18) gives the B.C. for Eq. (9) (Table 1). These results apply at clean reactor windows. This is an important observation because titanium dioxide adheres very easily to glass and quartz and appropriate corrections for fouling by the catalyst are necessary (see further ahead).

3.5. The VRPA with titanium dioxide

Solving Eq. (9) with its B.Cs. it is very simple to calculate

$$G_\lambda(x) = 2\pi \int_{\theta=0}^{\theta=\pi} I_\lambda(x,\theta)\sin\theta\,\mathrm{d}\theta. \tag{19}$$

Integration over the solid angle of irradiation eliminates the angular dependence of the transported radiation. For the one-dimensional—one directional model only integration on θ is required (Fig. 3). The LVRPA as a function of position and the reactor volume average of the LVRPA result:

$$e_\lambda^a(x) = \kappa_\lambda^{\mathrm{TiO_2}} G_\lambda(x), \tag{20}$$

$$\langle e_\lambda^a(x)\rangle_{V_R} = \frac{1}{L_R}\int_0^{L_R} e_\lambda^a(x)\,\mathrm{d}x. \tag{21}$$

The absorption coefficient has been assumed independent of position (uniform catalyst concentration) and time (stable catalyst). Calculating Eq. (21) we have the denominator of Eq. (1).

One may ask: how good is this method? Working with a bench scale, flat plate reactor and employing a two-dimensional—two-directional radiation model (reactor without azimuthal symmetry) it has been shown by Brandi, Alfano, and Cassano (2000), that the solution of the RTE with the discrete ordinate method, when the appropriate optical properties, phase function and boundary condition are used, provide values with an error smaller that 10% as compared with experimental, precise measurements. Unfortunately, accurate experimental data for all the outgoing photons due to out-scattering are very difficult to obtain (see Brandi et al., 1999, 2000). The numerical solution of the RTE [Eqs. (9)–(11)] is not simple but can be obtained in one standard PC with rather short computing times even for polychromatic radiation and more complex geometries.

4. Experiments

For measuring photocatalytic quantum yields at 313 and 365 nm the decomposition of two compounds have been chosen: 1-4 dioxane and phenol. They are typical representatives of aliphatic and aromatic pollutants and are commonly used as model compounds in photocatalytic and other advanced oxidation technologies studies. The experimental conditions are shown in Table 2. pH = 3 is very often selected for conducting these reactions and has the advantage of being separated from the isoelectric point of titanium dioxide in water; then, agglomeration of catalytic particles is minimized, a phenomenon that would change the optical properties of the system. Degussa P 25 is the most widely variety of titanium dioxide used in photocatalytic research.

The liquid (pure water, 1000 cm^3) was fed to the reacting system and saturated in situ with oxygen. Each one of the organic compounds was dissolved in pure water at the desired concentration, added to the tank and mixed with the

Table 2
Experimental conditions

Temperature	298 K
Initial pH	3.0
Solvent	Pure water
Oxygen (for saturation)	99.99% pure
Initial substrate concentration	20 ppm
Titanium dioxide variety	Degussa P 25
Catalyst concentration	2.0×10^{-3} g cm^{-3}

Table 3
Absolute quantum yield results

Absolute quantum yields (mol einstein^{-1})		
Compound	Wavelength (nm)	
	313	365
1,4-dioxane	0.0533	0.0399
Phenol	0.0949	0.0851

Table 4
Apparent quantum yield results

Apparent quantum yields (mol einstein^{-1})		
Compound	Wavelength (nm)	
	313	365
1-4-dioxane	0.0182	0.0106
Phenol	0.0316	0.0163

Table 5
Fraction of radiation scattered at the window of radiation entrance

Wavelength (nm)	$q_\lambda^{back}/q_\lambda^{wall}$
313	0.242
365	0.581

oxygen-saturated water. The initial concentration was measured. Afterwards the prescribed amount of catalyst was incorporated into the tank. Each catalytic suspension was subjected to ultrasound treatment for 30 min before its use in an experimental run. After 2 h of mixing by recirculation, 12 additional hours were allowed for reaching adsorption equilibrium between the substrate and the catalyst. The reaction starting concentration in the liquid (different from the initial one because of adsorption) was measured. Each run was initiated when the lamp operation, flow rates and temperatures were at steady state at the prescribed operating conditions (ca. 2 h).

Fouling of the reactor walls was properly measured with the calibrated radiometer. These measurements permitted to calculate the exact boundary condition for radiation entrance needed by the solution of the RTE. In this way the photon absorption rate at each reaction time corresponds to the actual window conditions that prevail at the moment in which reaction rates are experimentally measured. Concentration data were taken at prescribed time intervals and from the concentration vs. time plots reaction rates can be readily calculated. Employing monochromatic radiation, the available energy inside the reactor is never too high. In order to have meaningful changes in concentration, a normal run lasted between 12 and 16 h. Analysis of phenol (J.T. Baker, ACS) and 1,4-dioxane (Carlo Erba, RS) were made with HPLC (UV detector) and GC (FID detector), respectively.

5. Results

Values for absolute quantum yields are included in Table 3. At lower wavelengths quantum yield are higher. These results are in agreement with the fact that at lower wavelengths the excess energy with respect to the band-gap energy for the activation of the semiconductor is larger. Then this excess energy will operate against the recombination reaction of electrons and holes, a reaction that undoubtedly will reduce the quantum yield. These results can be compared with the values calculated for the apparent quantum yields computed in terms of the incident photons according to Eq. (2) (see Table 4).

It is interesting to know how many photons are lost from the reactor due to back-scattering at the window of radiation entrance exclusively. With Eq. (9) back-scattering in terms of incident radiation, at $x = 0$, can be calculated and compared with the known boundary condition produced by the actinometer experiments. Back-scattering is a function of the catalyst concentration for low catalyst loading (say below 0.5×10^{-3} g cm^{-3}). At the catalyst concentrations employed in these experiments, back-scattering is almost independent of the amounts of solid that are present; i.e., some sort of plateau has been reached beyond 0.5×10^{-3} g cm^{-3}. The results are illustrated in Table 5.

6. Conclusions

Resorting to mathematical modeling and the solution of the radiative transfer equation, and using a very simple reactor, monochromatic quantum yields for photocatalytic reactions carried out in slurry reactors can be accurately measured. The method can be extended to other reactions and other catalysts with no additional difficulties. It has also been shown that in a typical laboratory reactor (window with a diameter equal to 5.2 cm and length equal to 10 cm) apparent quantum yields differ from true quantum yields between 66% and 81% and that for the same geometric arrangement, back-scattering (that is often neglected) accounts for 24–58% of the incident radiation.

Acknowledgements

The authors are grateful to Universidad Nacional del Litoral, Consejo Nacional de Investigaciones Científicas y Técnicas, Agencia Nacional de Promoción Científica y Tecnológica and the CYTED program for their support to produce this work. Thanks are also given to Eng. Claudia M. Romani for technical assistance.

References

Brandi, R. J., Alfano, O. M., & Cassano, A. E. (1999). Rigorous model and experimental verification of the radiation field in a flat plate solar collector simulator employed for photocatalytic reactions. *Chemical Engineering Science*, *54*(13–14), 2817–2827.

Brandi, R. J., Alfano, O. M., & Cassano, A. E. (2000). Evaluation of radiation absorption in slurry photocatalytic reactors. 2. Experimental verification of the proposed method. *Environmental Science and Technology*, *34*(12), 2631–2639.

Cabrera, M. I., Alfano, O. M., & Cassano, A. E. (1996). Absorption and scattering coefficients of titanium dioxide particulate suspensions in water. *Journal of Physical Chemistry*, *100*(51), 20 043–20 050.

Cabrera, M. I., Negro, A. C., Alfano, O. M., & Cassano, A. E. (1997). Photocatalytic reactions involving hydroxyl radical attack II: Kinetics of the decomposition of trichloroethylene using titanium dioxide. *Journal of Catalysis*, *172*(2), 380–390.

Calvert, J. G., & Pitts, J. N. (1966). *Photochemistry*. New York: Wiley.

Cassano, A. E., Martín, C. A., Brandi, R. J., & Alfano, O. M. (1995). Photoreactor analysis and design: Fundamentals and applications. *Industrial Engineering Chemistry Research*, *34*(7), 2155–2201.

Duderstadt, J. J., & Martin, W. R. (1979). *Transport theory*. New York: Wiley.

Murov, S. L., Carmichael, I., & Hug, G. L. (1993). *Handbook of photochemistry* (2nd ed.). New York: Marcel Dekker.

Özisik, M. N. (1973). *Radiative transfer and interactions with conduction and convection*. New York: Wiley.

Siegel, R., & Howell, J. R. (1992). *Thermal radiation heat transfer* (3rd ed.). Washington, DC: Hemisphere.